Acta Biomed 2026; Vol. 97, N. 1: ISSN: 0392-4203 | eISSN: 2531-6745

SYNTHESIS OF MAGNESIUM NANOPARTICLE AND NANOCOMPOSITE IN EXTRA-CELLULAR FILTRATES FROM MICROBIAL CULTURES FOR WASTE DEGRADATION

Ofunnwa, J.O[1]. Ikele, M.O.[2,3], Oghonim, P. AN[4], Agu, K.C.[3], Egwuatu, C.I.[5], Obumselu, O.F.[5], Umeoduagu, N.D.[1], Awari, V.G.[1], Mbachu, I.A.C.[6], Anieto, E C.[7]

[1]Department of Microbiology, Tansian University, Umunya, PMB 0006, Anambra, Nigeria

[2]Department of Food, Nutrition and Packaging Sciences, College of Agriculture, Forestry and Life Sciences, Clemson University, South Carolina, 29634 USA

[3]Department of Applied Microbiology, Nnamdi Azikiwe University, P.M.B. 5025 Awka, Nigeria

[4]Microbiology Department, Biological Sciences, University of Delta, Agbor P.M.B 2090, Agbor, Delta State, Nigeria.

[5]Pure and Industrial Chemistry Department, Nnamdi Azikiwe University, P.M.B. 5025 Awka, Nigeria

[6]Department of Microbiology, Chukwuemeka Odumegwu Ojukwu University, Uli, Nigeria

[7]Department of Pharmaceutical Microbiology and Biotechnology, Faculty of Pharmaceutical Sciences, University on the Niger, KM-13, Onitsha - Enugu Express Way Umunya.

Corresponding author's e-mail: mo.ikele@unizik.edu.ng

ABSTRACT

Magnesium oxide nanoparticles are currently used for different environmental safety applications because they exhibit high ionic properties, high stability, biocompatibility, and high-contaminant adsorption; they are also safe and cost effective. Conventional methods of Magnesium oxide nanoparticle synthesis are known to have strong deleterious impact on the environment thus; microbial biosynthesis method gained more attention. This study synthesized magnesium nanoparticles from beneficial oligotrophic microbial cultures, and tested on solid waste degradation. Microbes were isolated from the soil, roots of soybeans, and ripe pineapple employing routine microbiology techniques, and assessed for their degradative capacities. Top three isolates with the best degradative index were made the choice isolates for nanoparticle production, and their identities were confirmed using molecular sequencing. Magnesium nanoparticles were synthesized from a blend of the choice isolates, and characterized using ultraviolet-visible (UV-VIS) spectrophotometric analysis, Fourier transforms (FTIR) infra-red, X-ray diffraction (XRD) investigation, and scanning electron microscopic (SEM). Synthesized nanoparticles were checked for their waste degradation potential through composting. *Enterobacter* sp., *Bacillus thuringiensis* and *Candida tropicalis* were the effective organisms identified using molecular sequencing. UV-VIS spectral profile of the microbially synthesized magnesium nanocomposite showed highest absorption peak of 1.08 was found at 500 nm, FTIR profile showed the highest broad and intense absorption peak was a wavenumber frequency region of 3715.104 cm^{-1}, X-ray diffraction showed diffraction-intense peaks in the spectrum of two-degree theta shift data ranging from 2° to 70°, and scanning electron micrograph showed that the

Acta Biomed 2026; Vol. 97, N. 1: ISSN: 0392-4203 | eISSN: 2531-6745

MgO nanocomposite was a dispersed, aggregated nano spherical sheet in shape. All the composting units had fine homogenous materials in texture, dark brown to black in colour, slightly foul to earthy smell in odour, 12.0, 7.2, 7.2, 5.5 cm in compactness (height) and 4.067, 2.595, 3.318, 2.648 kg in mass reduction for control, effective microorganisms, magnesium nanocomposite and consortium respectively, after the composting period.

Key words: Bio-composting, Magnesium nanoparticles, Magnesium nanocomposites, Nanomaterials.

1.0 INTRODUCTION

The science of nanoparticles has gained more interest and developing tremendously. Nanoscience synthesizes new materials (1–100 nanometers) within the nanoscale (Fazizadeh et al., 2016; Fernandes et al., 2020) which possess exceptional properties that are devoid of large materials. The use of nanoparticles in science is preferred for reasons of compatibility, surface charge, shape, size, catalytic activity, chemical stability, and small size to a large surface area (Cai et al., 2017). These features are essential for their integration into various biotechnological and medical applications. Different chemical, physical, and biological methods, have been employed to synthesize nanomaterial compounds (Foudda et al., 2021). Requiring high energy with tough experimental devices, the physical methods were accomplished under severe working, while the chemical production took place using harmful organic solvents with hazardous reducing agents, which synthesized unwanted by-products that negatively impacted the surrounding environment. Considering these limitations associated with the use of physical and chemical methods, the biological method of synthesizing nanomaterials (especially using saprophytic microorganisms) has received maximum interest in recent times (Hassan et al., 2021).

Among important metal oxide nanoparticles, such as magnesium oxide nanoparticles (MgO-NPs), research has shown that they exhibit high ionic properties, high stability, biocompatibility, cost-effectiveness, a crystal structure, safe and high-contaminant adsorbents (Cai et al., 2017; Opetubo et al., 2025). MgO-NPs various applications and exceptional features have made them highly preferable to other metal oxide nanoparticles by researchers globally for the past two decades (Khan et al., 2020). Magnesium oxide nanoparticles and their composites are currently being used for different environmental safety applications such as pesticide detection, heavy metal detection, pesticide degradation, removal of waste water contaminants and waste degradation (Gatou et al., 2024). MgO-NPs have found new uses in the biomedical, sensing, adsorbent, lithium battery, refractory materials, wastewater treatment, ceramics, heavy fuel oils, removal of toxic waste, catalysis, antimicrobial qualities, and the agriculture, biomedical, and ferroelectric thin-film industries (Hornak, 2021; Hassan et al., 2021).

Several researchers have claimed that MgO-NPs can be produced using a variety of techniques, such as solvent modification, co-precipitation, moist chemical, sol-gel, and hydrothermal processes; however, these techniques have extremely negative environmental impacts (Duong et al., 2019; Khan et al., 2020). The biological synthesis of nanoparticles using fungi is recently

becoming the preferable method because of the flexibility of handling, high growth rates, species diversity, cost-effectiveness, novelty, and eco-friendly potentials. Either the transport of metal ions inside the fungal cell and subsequent reduction by enzymes (intracellular method) or the reaction of metal ions with fungal biomass filtrate (extracellular method) can be used to synthesize MgO-NPs with fungi as the organisms carries out biodegradation activities (Bhardwaj et al., 2020). Microorganisms involved in waste decomposition possess remarkable degradative capacities, largely due to their ability to produce extracellular enzymes such as cellulases, lipases, mannanases, ligninases, and other hydrolytic enzymes (Agu et al., 2013; Agu et al., 2014a; Agu et al., 2014b; Orji et al., 2014; Anaukwu et al., 2016a). Through the production and secretion of these enzymes, both fungi and bacteria play crucial roles in biodegradation by breaking down complex organic materials into simpler compounds that can be readily assimilated and recycled within the environment (Mbachu et al., 2014; Anaukwu et al., 2016b; Agu & Odibo, 2021; Orji et al., 2022; Agu et al., 2022; Okeke et al., 2023; Egurefa et al., 2024).Biodegradation capacities of these microbes give rise to the synthesis of other biological compounds which includes useful nanoparticles like the MgO-NPs.

Metallic nanoparticles (silver, mercury, iron, selenium, magnesium) have been reported by several researchers to be synthesized through intra-cellular methods by certain microbes (*Bacillus* species, *Saccharomyces* species) used in waste composting/degradation, and treatment of water (Jeevan

Adam et al. (2017), Cai et al. (2017), Alam et al. (2019), and Fernandes et al. (2020)); however, little information has been documented on the synthesis of magnesium nanoparticles and nanocomposite from biodegrading microorganisms. Thus, this study sought to synthesize magnesium nanoparticles and nanocomposites from beneficial microbial culture blends (bacteria and fungi), and test the capacity of the synthesized magnesium nanoparticles in waste degradation.

2.0 MATERIALS AND METHODS

Isolation of Rhizospheric Bacterial (RB) Species

According to the method of Ogbo and Okonkwo (2012), 3 cm segments of the washed roots of soybean plants were cut and disinfected by soaking in 70 ethanol for 5 min, and in 6.25% sodium hypochlorite for 10 min. Afterward, the roots were rinsed severally with sterile water. Root pieces (0.5 to 1.0 cm), which were intact, were placed into tubes of semi-solid (0.05%) nitrogen-free biotin medium (NFb) and incubated without shaking for 5 days at 30ºC. This medium was composed (g/L) of: DL-malic acid 5; KOH 4; K_2HPO_4 0.5; $MgSO_4 \cdot 7H_2O$ 0.2; $CaCl_2$ 0.02; NaCl 0.1; $FeSO_4 \cdot 7H_2O$ 0.5; Agar 5 g; and (mg/L) of: $NaMoO_4 \cdot 2H_2O$ 2; $MnSO_4 \cdot H2O$ 10. The medium also contained 2 mL of a 0.5% solution of bromothymol blue in 95% ethanol and had a final pH of 6.8. After incubation, the white pellicles from tubes with this characteristic feature were sub-cultured onto solid semi-selective, Congo red-NFb medium. Colonies with red to scarlet appearance (suggestive of the rhizospheric bacterium) were selected and isolated to pure cultures by repeated streaking on the same medium.

Isolation of Yeast

Acta Biomed 2026; Vol. 97, N. 1: ISSN: 0392-4203 | eISSN: 2531-6745

Pineapple fruits were washed with distilled water, drained, peeled, and sliced into smaller pieces. The juices were extracted aseptically using a hand juice extractor, filtered with a muslin cloth, and the filtrates were collected in a sterile plastic container as described by Umeh et al. (2019). Thereafter, 100 mL of Yeast Extract Dextrose Peptone Broth (40 g of peptone water, 10 g of yeast extract, and 20 g of sucrose in 1 L of distilled water) was added into a 250 mL conical flask containing 100 g of the 48-hour fermenting crushed pineapple, respectively, and were incubated for 2–5 days at 30 °C to enhance microbial growth for the isolation of yeast. A 0.1 mL aliquot of the YEDP broth containing the pineapple juice was inoculated in a Potato Dextrose Agar (PDA) medium (50 mg/L of tetracycline and 0.05 mg/L of gentamycin were added to the PDA medium to inhibit bacterial growth) in duplicates using a glass spreader. For 72 h, plates were incubated at 30 °C. The colonies on the plates were further sub-cultured and incubated for another 48 h at 30 °C to obtain pure cultures. The selected yeast isolates were obtained, and the pure cultures of the isolates were stored in Bijou bottles with 10% glycerol at 4 °C (Alabere et al. 2020).

Screening of organisms with High Degradative Activity

According to the method of Zhao *et al.* (2017) and Limaye *et al.* (2017) retrieved isolates were inoculated (100 µL) into starch, fat, protein, lignin and cellulose containing media. The starch medium (1000 mL) comprised soluble starch 2 %, NaCl 0.5 %, peptone 0.5 %, and agar 2 %; the fat medium (1000 mL) comprised peptone 1 %, NaCl 1 %, $CaCl_2 \cdot 7H_2O$ 0.01 %, Tween-80 1 % and agar 2 %, pH 7.4 – 7.8; the protein medium (1000 m L) comprised non - fat dried milk 5 % and agar 1.8 %; lignin medium (1000 mL) comprised $(NH_4)_2SO_4$ 0.2 %, K_2HPO_4 0.1 %, KH_2PO_4 0.05 %, $MgSO_4$ 0.02 %, yeast extract 0.1 %, maltose 0.02 %, asparagine 0.02 %, agar 2.3 % and 0.01 % guaiacol dissolved in ethanol. Sterile trace solution ($CuSO_4 \cdot 7H_2O$ − 0.01 %, $ZnSO_4 \cdot 7H_2O$ 0.03 %, $MnCl_2 \cdot 5H_2O$ 0.02 %, MgSO4·$7H_2O$ 0.25 %, $CaCl_2 \cdot 2H_2O$ 0.15 %, $FeSO_4 \cdot 7H_2O$ 0.03 % and $COCl_2 \cdot 6H_2O$ 0.01 %) 0.1 % v/v was added to the lignin medium after autoclaving and the cellulose medium (1000 mL) comprised K_2HPO_4 0.1 %, carboxyl methyl cellulose 0.5 %, $MgSO_4$ 0.05 %, glucose 0.1 %, yeast extract 0.05 %, $NaNO_3$ 0.1 %, KCl 0.1 % and agar - agar 2.2 %. All the plates were incubated for 5 days at room temperature. The presence of clear zones around each colony was indicative of degradation activity. Additionally, iodine was added to the starch medium and neutral red dye was also added to the fat medium to enhance colour contrast. The lignin medium was covered with 0.5 % of methyl orange dye solution while cellulose agar surface was covered with 0.1 % Congo red solution for 15 minutes and the plate was overlaid with 1 M NaCl for 1 h. In triplicates, the degradative activity was measured and the mean subsequently calculated. Strains with the highest degradative activity were made choice isolates for Magnesium nanoparticle production and composting experiments.

Identification of Isolates with best degradative activity

16s rDNA and ITS-region sequencing were used to identify the choice isolates, after DNA extraction and purification has been carried out.

Extracellular Biosynthesis of Magnesium Nanoparticle/Nanocomposite

Inoculum preparation

Acta Biomed 2026; Vol. 97, N. 1: ISSN: 0392-4203 | eISSN: 2531-6745

Each bacterial/yeast culture was inoculated in a 250-mL conical flask containing 200 mL of sterile nutrient broth and YEDP broth for the inoculum preparation. The flask was incubated at 28 °C for 48 h (bacteria) and 120 h (yeast) on a rotary shaker at 150 rpm; the cells were harvested by centrifugation at 4,000 rpm for 20 min, and the collected cell pellets were dried in a hot air oven at 60 °C for 24 h (Namasivayam et al. 2010; Kaul et al. 2012).

Preparation of Cell Filtrate Suspension

The dried cell pellets were washed twice using deionized water, and the washed cell pellets were transferred to 250 mL of a conical flask containing 100 mL of deionized water and kept on a rotary shaker at 180 rpm for 24 h (bacteria) and 72 h (yeast). After the incubation, the mixture was centrifuged, and the upper layer (supernatant) was collected and used for the biosynthesis of MgO-NPs (Saied et al., 2021; Kaul et al., 2012). The bacterial and yeast suspensions from the various tubes were mixed in 1:1:1 ratio in a 100-mL conical flask to form a suspension blend for nanoparticle production (Kaul et al. 2012).

Magnesium Nanoparticle and Nanocomposite Biosynthesis

The modified methods of Kazemi et al. (2020), Hassan et al. (2021), and Saied et al. (2021) were adopted in the biosynthesis of magnesium nanoparticles and nanocomposites. In this method, 0.8 g of gelatin was firstly dissolved in 10 mL of 4 mM aqueous solution of Mg $(NO_3)_2.6H_2O$ (approximately 102.5 mg of Mg $(NO_3)_2.6H_2O$ in 10 mL distilled water (H_2O)) and then stirred for 120 min using a magnetic stirrer at 70 °C and 80 rpm to form a homogenous suspension. The gelatin-magnesium nitrate mixture was then mixed with 90 mL of all bacterial and fungal biomass filtrates on a magnetic stirrer overnight until color change. At the end of the incubation period, the Mg $(OH)_2$ was formed as a turbid white precipitate, which was collected and rinsed with distilled water to remove any impurities before being oven-dried at 100 °C for 1 h.

The formed Mg $(OH)_2$ was calcinated at 400 °C for 3 h to form MgO-NPs, as represented in Equation (1).

$$Mg(OH)_2 \xrightarrow{400\ ^\circ C} MgO - NP_5 \quad \text{.....(1)}$$

Physical and Chemical Characterization of Magnesium Oxide Nanoparticle and Nanocomposite (MgONCPs)

UV-VIS spectrophotometric

On the nanoparticle samples, UV-visible spectrophotometric analysis was conducted at the Center for Energy Research and Training (CERT) in Zaria, Nigeria, using a UV-visible spectrophotometer (Apel 3000UV) with a slit 2 nm width, using a 10-mm cell at room temperature. The produced MgONCPs were examined under visible and UV light in the wavelength range of 200–1100 nm (Wang et al. 2014; Fazlzadeh et al. 2016).

Fourier transform infrared (FTIR) spectroscopic analysis.

The Fourier transform infrared (FTIR) spectroscopic analysis was carried out at the Center for Energy Research and Training (CERT) in Zaria, Nigeria, to determine the functional groups of

Acta Biomed 2026; Vol. 97, N. 1: ISSN: 0392-4203 | eISSN: 2531-6745

produced MgONCPs using Buck Scientific M530 USA FTIR for the analysis. This instrument which had a deuterated triglycine sulfate detector, and a beam splitter of potassium bromide was equipped. The software of Gram A1 was used to obtain and manipulate the spectra. Zero point five milliliters (0.5 mL) was approximately 1.0 g of samples, mixed properly, and placed on the salt pellet. During measurement, FTIR spectra were obtained at frequency regions of 4,000–600 cm1 and co-added at 32 scans and 4 cm1 resolution, as transmitter values FTIR spectra were displayed (Wang et al. 2014; Fazlzadeh et al. 2016).

X-ray diffraction (XRD) analysis

The phase purity and crystalline nature as well as the X-ray diffraction patterns of the produced MgONCPs were determined at the Center for Energy Research and Training (CERT) in Zaria, Nigeria, using an X-ray diffractometer (Philips X-ray Analytical, Amsterdam, The Netherlands). The samples for analysis were prepared by pressing the powder into the cavity of a sample holder and smoothing it with a glass slide. They were scanned from 5° to 70° 2θ with a Cu anode X-ray operated at 40 kV and 40 mA in combination with a Ni filter to give a monochromatic Cu-Kα radiation (λ = 1.5418 Å) (Wang et al. 2014a; Fazlzadeh et al. 2016). The average nanocomposite sizes were calculated using Equation 2 proposed by Hassan et al. (2021).

$D = K\lambda / \eth \cos\vartheta$ .....Equation(2)

Where D is the average particle size, K is the Scherrer's constant (0.9), λ is the wavelength of X-ray radiation (0.1542 nm), and β and θ are half of the maximum intensity and Bragg's angle, respectively.

Scanning electron microscopic (SEM) analysis

The sizes and morphologies of the produced MgONCPs were determined at the Center for Energy Research and Training (CERT) in Zaria, Nigeria, using a scanning electron microscope (SEM) Quanta FEG 450 (FEI) (APOLLO X-EDAX). Zero-point five-gram (0.5 gram) samples were coated with Au/Pd film, and the SEM images were obtained using a secondary electron detector. Point chemical analysis was performed on 2 independently selected particles (Wang et al. 2014a; Fazlzadeh et al. 2016).

Evaluation of Synthesized Magnesium Nanoparticles in Waste Degradation

Composting unit

The passive aeration composting experiment was carried out in 13 L laboratory made plastic bin composter with dimensions 43 cm x 32 cm x 25 cm (length x width x height) and aeration holes (0.6 cm diameter) at the sides of the bin. Each experiment contained 5.5 kg shredded and dried final waste mixture of approximately 55% food waste, 15% saw dust waste, grass chopping waste 22 % and 8% paper with or without inoculation as described by Aslanzadeh *et al*. (2019). The first set up was added a blend of bacterial and yeast suspension, the second set up was magnesium nanoparticles labelled Mg nanocomposite, the third set up was added a combination of both microbial blends and magnesium nanocomposite labeled consortium while the fourth set up labelled uninoculated control was maintained with saline of 0.01 % Tween -80, respectively (Zhao *et al.* 2017; Saleh *et al.* 2020).

Acta Biomed 2026; Vol. 97, N. 1: ISSN: 0392-4203 | eISSN: 2531-6745

Composting units were kept in the laboratory shade. Composting was allowed to take place for 8 weeks. Moisture level was maintained by addition of 20 mL sterile water to the pile every day. All the samples were aerated by turning the pile using sterile plastic rod every day in the first two weeks and after that only once a week for the rest of the experimental period. The experiment was carried out in triplicates (Limaye *et al.* 2017; Aslanzadeh *et al.* 2020).

The texture, colour, odour, compactness **(**height) of the compost pile set ups were determined at the beginning and end of the composting using calibrated meter rule and values were recorded in centimeter scales (Limaye *et al*., 2017). The percentage in compost height or compactness was determined. Also, the whole composted samples were weighed using weighing balance every 2 weeks for 8weeks and the percentage of mass loss or reduction was determined (Zhao *et al*., 2017).

Statistical Analysis

Data were analyzed using GraphPad Prism Version 8.0.2. Descriptive statistics were performed to summarize the data in mean and standard deviation. One way ANOVA was also used to test for significance at 95% confidence interval.

RESULTS

Degradation Profile of Microbial Strains

Three isolates gave the most enzyme activity profile and were selected as choice isolates for characterization and composting. The results of the colony diameter, clearance zone from their enzyme activity indices of are shown in Table 1.

Table 1: Enzymatic Degradation Profile of Choice Isolates

Isolate Code	Amylase Activity Diameter clear Zone (mm)	Protease Activity Diameter clear zone (mm)	Cellulase Activity Diameter clear Zone (mm)	Ligninase Activity Diameter clear zone (mm)
Y3	13.00±2.16	0.00±0.00	9.33±0.58	27.00±3.79
PSB2C	10.00±0.82	16.67±5.86	11.33±0.58	21.33±1.15
PSB1B	11.00±1.41	0.00±0.00	15.70±3.05	16.33±0.58

Molecular characterization of Choice Isolates

Table 2 shows the blast profile of 16S rRNA gene sequences from National Centre for Biotechnology Information (NCBI). The result identified the choice isolates as *Candida tropicalis*, *Bacillus thuringensis,* and *Entrobacter* sp.

Table 2: Blast profile of 16S rRNA gene sequences from National Centre for Biotechnology Information (NCBI)

Isolate code	Mole - cular ID NO	Description	Scientific name	Max	Total	Query	E Value	% ID	Acce-	Accessi - on

Acta Biomed 2026; Vol. 97, N. 1: ISSN: 0392-4203 | eISSN: 2531-6745

				score	score	Cover (%)		ssion length	NO from GenBank
PsB 1b	4_907-R_B07_04.ab1	*Enterobacter* sp. strain BAB-5981 16S ribosomal RNA gene, partial sequence	*Entero ba-cter* sp.	1214	1214	99	0.0	93.06	1401	KX548942.1
PSB 2c	6_785F_C11_08.ab1	*Bacillus thuringiensis* strain D456 16S ribosomal RNA gene, partial sequence	*Bacillus thuringie-nsis*	1144	1144	100	0.0	98.49	1422	ON939710.1
Y3	8_ITS1_F10_16.ab1	*Candida tropicalis* isolate S75AF internal transcribed spacer 1, partial sequence	*Candida tropicalis*	797	797	100	0.0	94.83	503	KY112741.1

Physico-Chemical Profile of Microbiologically Synthesized Magnesium Nanocomposite

Figure 1 represents the UV-VIS spectral profile of the microbially synthesized magnesium nanocomposite. From the result, the highest absorption peak of 1.08 was found at 500 nm, while the lowest peak of 0.027 was found at 600 nm. Figure 2 represents the FTIR profile of the

Acta Biomed 2026; Vol. 97, N. 1: ISSN: 0392-4203 | eISSN: 2531-6745

microbially synthesized magnesium nanocomposite when FT-IR analysis was scanned at a wavelength between 600 and 4,000 cm1. The results reveal the highest broad and intense absorption peak was a wavenumber frequency region of 3715.104 cm^{-1}, while the least was found around 719.1272 cm^{-1}, respectively. Figure 3 represents the X-ray diffraction patterns of microbially synthesized magnesium nanocomposite. Several diffraction-intense peaks in the spectrum of two-degree theta shift data ranging from 2° to 70°, respectively, were obtained. Figure 4 represents the scanning electron micrograph of microbially synthesized magnesium nanocomposite (3500x). The result revealed that the MgO nanocomposite was a dispersed, aggregated nano spherical sheet in shape.

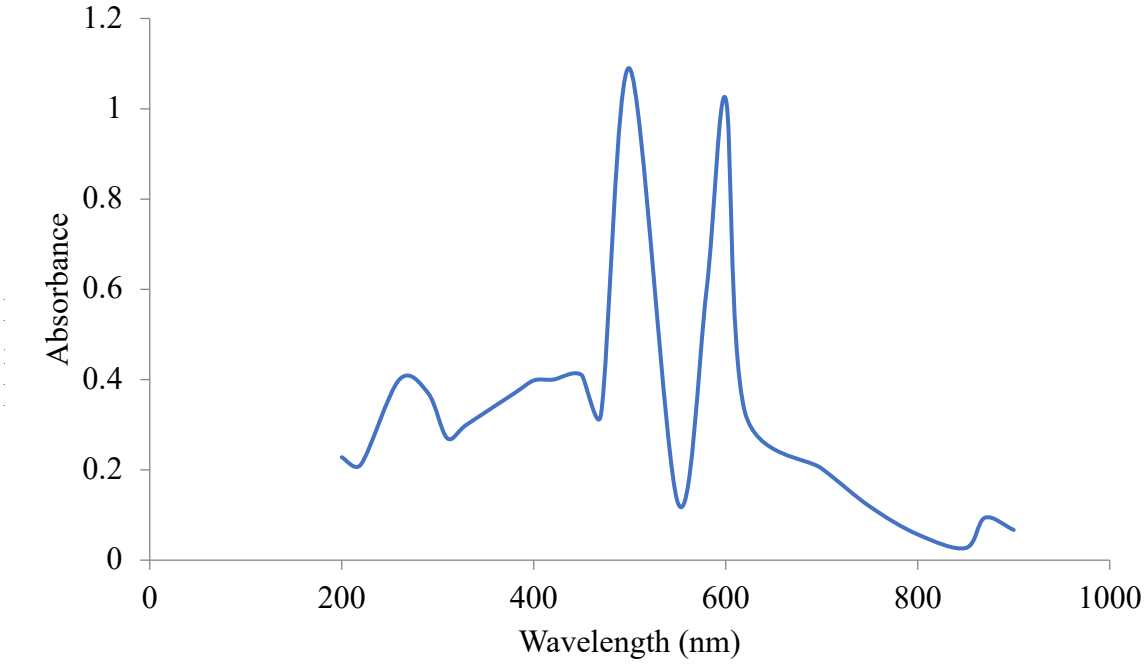

esium

Acta Biomed 2026; Vol. 97, N. 1: ISSN: 0392-4203 | eISSN: 2531-6745

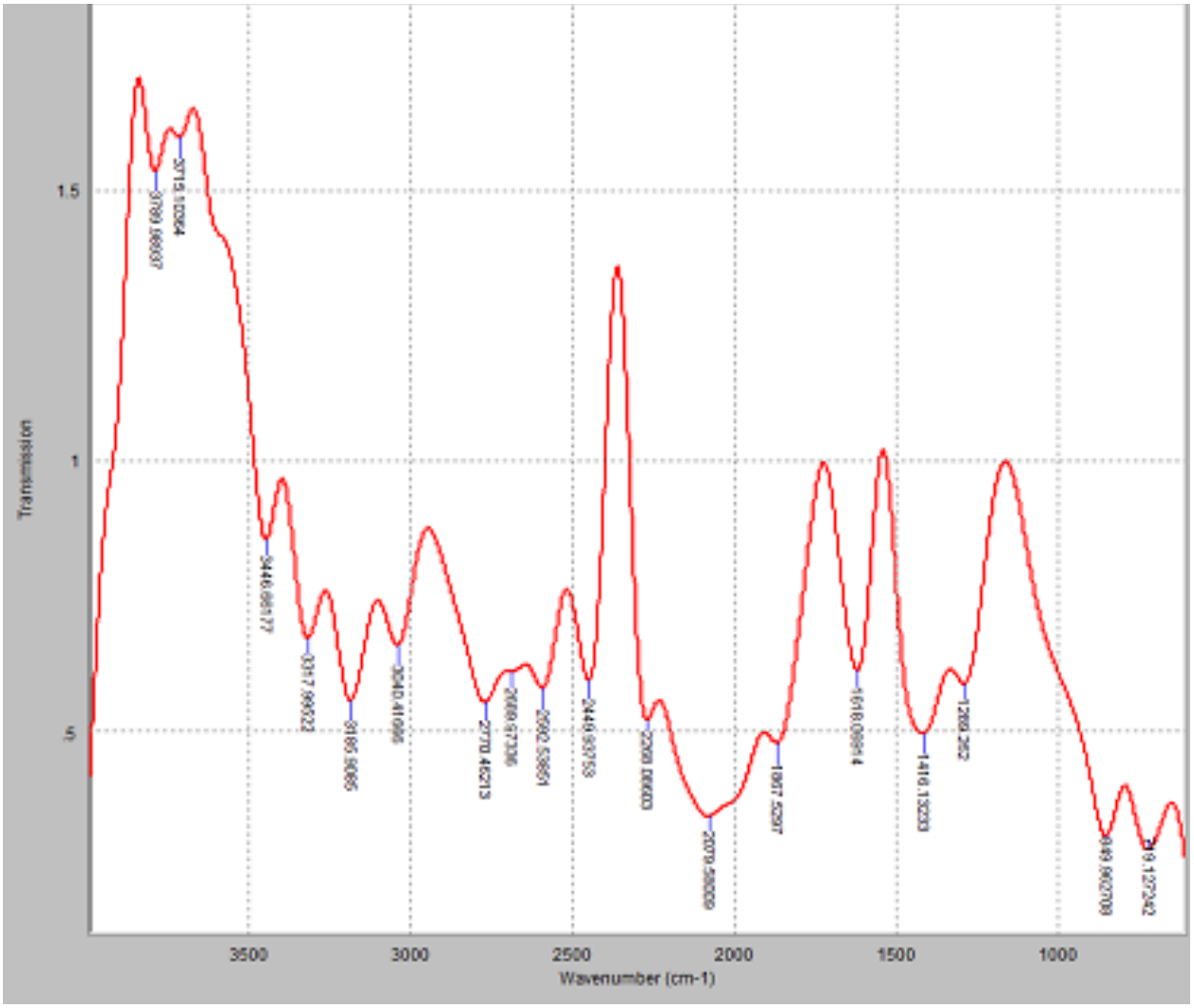

Figure 2: FTIR profile of the microbiologically synthesized magnesium nanocomposite
Key: cm^{-1}= Per centimetre

Acta Biomed 2026; Vol. 97, N. 1: ISSN: 0392-4203 | eISSN: 2531-6745

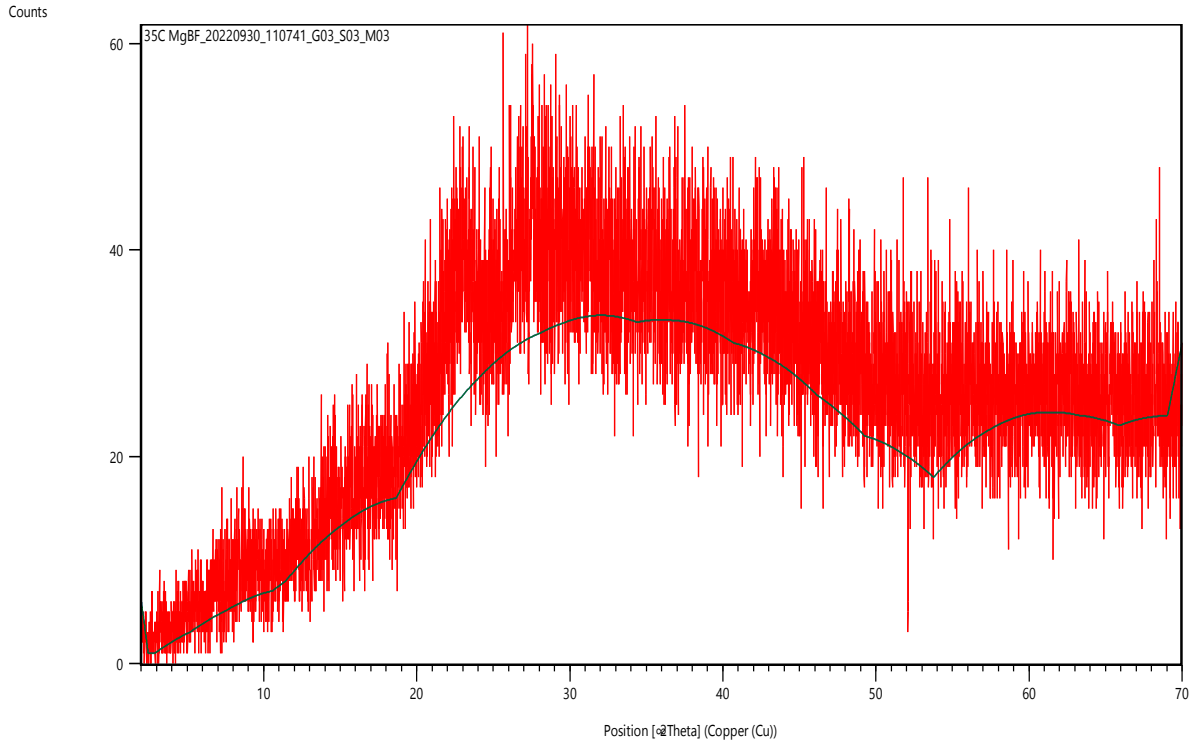

Figure 3: X-ray diffraction patterns of microbiologically synthesized magnesium nano-composite

Acta Biomed 2026; Vol. 97, N. 1: ISSN: 0392-4203 | eISSN: 2531-6745

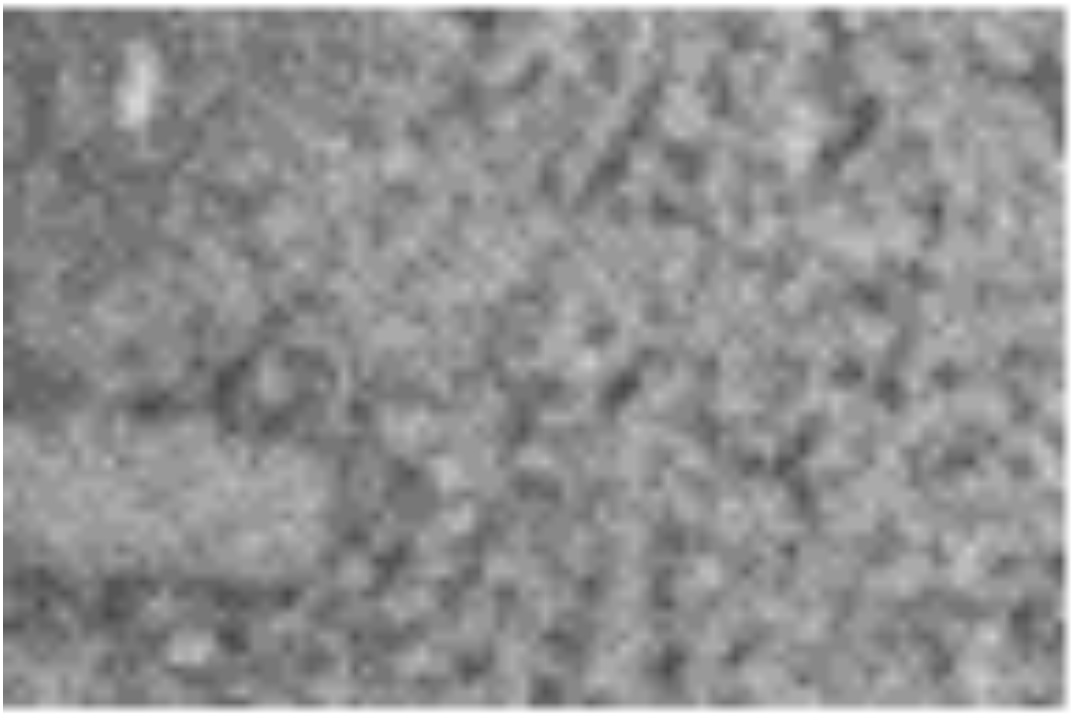

Figure 4: Scanning electron micrograph of microbiologically synthesized magnesium nanocomposite (3,500x)

Physical Profile of the Composted Material

Table 3 represents the changes in the physical parameters of composted materials before and after 56 days of composting period. All the composting units had fine homogenous materials in texture, dark brown to black in colour, slightly foul to earthy smell in odour, 12.0, 7.2, 7.2, 5.5 cm in compactness (height) and 4.067, 2.595, 3.318, 2.648 kg in mass reduction for control, effective microorganisms, magnesium nanocomposite and consortium after the composting period.

Table 3: Changes in the physical parameters of composted materials before and after composting period

Compost unit	Initial	Final
	Texture	
Control	Course heterogenous material	homogenous material
Effective microorganisms	Course heterogenous material	Fine homogenous material
Magnesium nanocomposite	Course heterogenous material	Fine homogenous material

Acta Biomed 2026; Vol. 97, N. 1: ISSN: 0392-4203 | eISSN: 2531-6745

Consortium	Course heterogenous material		Fine homogenous material
		Colour	
Control	Brown		Dark brown
Effective microorganisms	Brown		Black
Magnesium nanocomposite	Brown		Black
Consortium	Brown		Black
		Odour	
Control	Foul smell		Slightly foul smell
Effective microorganisms	Foul smell		Earthy smell
Magnesium nanocomposite	Foul smell		Earthy smell
Consortium	Four smell		Earthy smell
		Compactness (Height) (cm)	
Control	19.00		12.00
Effective microorganisms	18.80		7.20
Magnesium nanocomposite	19.20		7.20
Consortium	19.10		5.50 (*p*-value 0.0044)
		Mass reduction (kg)	
Control	5.500		4.067
Effective microorganisms	5.500		2.595
Magnesium nanocomposite	5.500		3.318
Consortium	5.500		2.648 (*p*-value 0.0065)

DISCUSSION

The result in Table 1 revealed that three strains namely PSB1b, PSB2c and Y3 out of the thirteen beneficial microbial strains demonstrated dormant amylase, protease, cellulose, ligninase and lipase enzymatic catalytic activities on different and were finally selected as effective microorganisms or microbial consortium for this study. The diverse metabolic abilities of these three microbial strains on carbohydrate, protein, cellulose, lignin and lipid substrates revealed that

Acta Biomed 2026; Vol. 97, N. 1: ISSN: 0392-4203 | eISSN: 2531-6745

these strains could acts as good decomposers, effective microbes and microbial additives in any composting technology. Table 2 revealed the strains were *Enterobacter* sp., *Bacillus thuringensis* and *Candida tropicalis.*

Recently, the biological synthesis of metal and metal oxide nanoparticles has developed growing interest due to their advantages over chemical and physical synthesis. The biomass filtrate of potent microorganisms after screening, was utilized to form MgO nanocomposite, as demonstrated by a color change from colorless to turbid white as shown in this study. This color change could be attributed to the enzymes and metabolites produced in the biomass filtrate, which reduced magnesium nitrate to magnesium hydroxide, and then to magnesium oxide (Hassan et al., 2021; Saeid et al., 2021). To further characterize the synthesized MgO nanocomposite particles, the ultraviolet spectroscopy technique was employed to monitor the color change and identify the maximum surface plasmon resonance (SPR), as a positive correlation exists between SPR and the shape, size, and distributed nanoparticles (Hassan et al., 2021). The result in Figure 1 revealed that the maximum SPR of the biogenic magnesium nanocomposite was detected at 500 and 600 nm, respectively. The reason for this observation was due to the isotropic feature of the nanocomposites. Jeevanandam et al. (2017) and Nguyen et al. (2021) explains that the size of biosynthesized MgO-NPs tends to be small when the SPR is less than 300 nm, which became more anisotropic at SPR greater than 300 nm.

FT-IR analysis is a potent technique used for detecting the likely functional groups present in the biomass filtrate of the potent microbial strains RB1, PSB2c, and Y3 that are responsible for the bio-reduction of metal precursors to form MgO-NPs (Saied et al., 2021). The result in Figure 2 revealed that the peaks around wavenumbers 3709.909–3715.104 cm^{-1} indicate mono-coordinated hydroxyl (-OH) groups. The peaks around wavenumbers 3317.995–3448.662 cm^{-1} indicate the presence of H bonds, while peaks close to 1416.132 cm^{-1} denote the bending vibration of the -OH groups of physically adsorbed water molecules may be visible (Hornak, 2021). Previous studies reported the successful synthesis of Mg-O nanocomposites at peaks around wavenumbers between 400 and 700 cm^{-1} (Pugazhendhi et al., 2019; Fouda et al., 2021; Hassan et al., 2021; Saeid et al., 2021). The detection of these functional peaks in the FT-IR spectra, which represent the metabolites from the biomass filtrate of the potent microorganisms, revealed their role in the bio-reduction and bio-stabilization of MgO-NPs (Hassan et al., 2021).

The XRD technique determined the magnesium nanocomposite purity phase and crystalline structure. In this study, the result in Figure 3 revealed that there are seven intense peaks at 2θ° values of 33.0°, 38.0°, 41.5°, 52.0°, 59.0°, 61.5°, and 68.90°. The XRD spectra data of the biogenic magnesium nanocomposite were compared to the crystallographic structure of the JCPDS standard (JCPDS file No. 89-7746) and confirmed to be nanocrystalline structures containing oxide in the form of Mg (OH)2 and MgO, respectively. Similar observations were reported by Diachenko et al. (2016), Hassan et al. (2021), and Hornak (2021), who obtained five intense peaks at 2θ of 36.9°, 42.6°, 62.2°, 75.4°, and 78.6° describing the crystalline structures of $Mg(OH)_2$ and MgO, respectively. The SEM analysis is considered a valuable technique in studying the topographical structure and aggregation of biosynthesized MgO-NPs (Hassan et al., 2021). The result in Figure

Acta Biomed 2026; Vol. 97, N. 1: ISSN: 0392-4203 | eISSN: 2531-6745

4 revealed that the microbiologically synthesized magnesium oxide nanocomposite was well dispersed and partly spherical with aggregation. Similar observations were reported in the published works of Hassan et al. (2021) and Saeid et al. (2021), but without aggregation in the microstructure of their biosynthesized MgO-NPs.

In this study, the bio-composting and biodegradation rates of solid wastes using effective microbial blends and their synthesized magnesium oxide nanocomposite were assessed using physico-chemical analyses of the composted material. Some authors (Kaul et al., 2012; Saied et al, 2021) reported that an increase in degradation rate and efficiency can be achieved by Effective Microorganisms (EM) by creating suitable environmental conditions for proper decomposition of organic materials used. The microbial activity is usually influenced by the particle size of the feedstock material, pH, moisture content, temperature, height of compost bed as well as other physicochemical and biochemical factors (Pushpa *et al*., 2016). In this study, the physico-chemical parameters were used for the preliminary characterization and monitoring of the composting materials during 56 days composting period. The result in Table 3 shows that all the composting materials in both treated and control composting units were fine and homogenous in texture, dark brown to black in colour, slightly foul to earthy smell in odour. These changes in texture and colour of the composted materials indicate the maturation of the final compost while the earthy smell odour indicates the absence of anaerobic conditions and is in agreement with the published work of Karanja *et al*. (2019) who reported all the composting materials showed temperature stability, pleasant earthy smell, fine texture, much darker brown to black colour, and homogeneity of materials, by the 62^{nd} day of composting. Likewise, there were significant ($P < 0.05$) percentage decrease in compactness (height) of control (36.80 %), effective microorganism (64.40 %), magnesium nanocomposite (62.5 %) and consortium (71.73 %), respectively after 56 days of composting which indicates the decomposition has taken place at constant rates. Previous study by Pushpa *et al*. (2016) reported that the height of the compost bed or compactness or height substantially decreased with increase in decomposition rate until the bed height was no longer reduced due to the maturity of compost. Similarly, there were significant ($P < 0.05$) percentage decrease in mass reduction of control (26.05 %), effective microorganism (52.82 %), magnesium nanocomposite (39.67 %) and consortium (51.85 %), respectively after 56 days of composting which also indicates that microbial decomposition took place at continuous rates. The substantial decrease in mass loss could further be explained to be a result of abundant nutrients and vigorous microbial metabolism at the initial stage of composting, which resulted in a rapid mass loss. Likewise, the decomposable organic matter was degraded by microorganisms, which possibly caused an exhaustion of the available carbon and nitrogen sources therein leading to possible mineralization (Zhao *et al*., 2017). Previous study by Zhang *et al*. (2013) reported that microbial metabolic activity was the primary reason for organic waste mass loss. In other words, microbes decomposed the organic components into micro-molecules and produced large amounts of CO_2, which thus buttresses the observation made in this study.

Conclusion

The study has shown that microorganisms can produce magnesium nanoparticles due to their ability to synthesize enzymes that convert magnesium sulfate to magnesium hydroxide and, finally, to magnesium (ii) oxide. The biosynthesis of magnesium nanoparticles in this study was confirmed and evaluated using UV-VIS, FTIR, XRD, and SEM. The produced magnesium nanoparticles are likewise useful in solid waste composting.

Conflict of Interest

Authors declare no conflict of interests.

Funding Statement

This study did not receive any external funding.

Authors' contributions

Conception: Ofunwa, Agu; Planning: Umeoduagu, Awari; Execution: Ofunwa, Oghonim, Egwuatu; Writing: Ikele, Agu; Interpretation: Ikele, Ofunwa, Obumselu, Mbachu; Statistical analyses: Ikele, Anieto.

REFERENCES

Agu, K. C., & Odibo, F. J. C. (2021). Biodegradation potentials of *Aspergillus flavipes* isolated from Uburu and Okposi salt lakes. *International Journal of Trend in Scientific Research and Development, 5*(5), 1160–1170. https://www.ijtsrd.com/papers/ijtsrd44949.pdf

Agu, K. C., Ogbue, M. O., Abuchi, H. U., Onunkwo, A. U., Chidi-Onuorah, L. C., & Awah, N. S. (2013). Lipase production by fungal isolates from palm oil-contaminated soil in Awka, Anambra State, Nigeria. *International Journal of Agriculture and Biosciences, 2*(6), 386–390.

Agu, K. C., Okafor, F. C., Amadi, O. C., Mbachu, A. E., Awah, N. S., & Odili, L. C. (2014a). Production of mannanase enzyme using *Aspergillus* spp. isolated from decaying palm press cake. *Scholars Academic Journal of Biosciences, 2*(12A), 863–870.

Agu, K. C., Orji, M. U., Ikele, M. O., Uwanta, L. I., & Onyeneho, V. I. (2022). Hydrocarbon biodegradation potential of cyanobacteria in oil polluted soil. *International Journal of Trend in Scientific Research and Development, 6*(7), 733–737. https://www.ijtsrd.com/papers/ijtsrd52397.pdf

Agu, K. C., Orji, M. U., Onuorah, S. C., Egurefa, S. O., Anaukwu, C. G., Okafor, U. C., Awah, N. S., Okafor, O. I., Mbachu, A. E., & Anyaegbunam, B. C. (2014b). Influence of solid waste dumps leachate on bacteriological and heavy metals contamination of groundwater in Awka. *American Journal of Life Science Researches, 2*(4), 450–457.

Alabere, A., Ogbonna, D. N., & Williams, J. O. (2020). Screening of yeast cells for the production of wine from banana and pineapple substrates. *Journal of Advances in Microbiology, 20*(7), 38–55.

Alam, H., Khatoon, N., Khan, M. A., Husain, S. A., Saravanan, M., & Sardar, M. (2019). Synthesis of selenium nanoparticles using probiotic bacteria *Lactobacillus acidophilus* and their enhanced antimicrobial activity against resistant bacteria. *Journal of Cluster Science.*

Anaukwu, C. G., Ezemba, C. C., Anakwenze, V. N., Agu, K. C., Amechi, S. N., Okeke, B. C., & Awah, N. S. (2016a). Influence of anionic, cationic and non-ionic surfactants on growth of hydrocarbon-utilizing bacteria. *American Journal of Current Microbiology, 4*, 10–16.

Anaukwu, C. G., Ezemba, C. C., Anakwenze, V. N., Agu, K. C., Okeke, B. C., Awah, N. S., & Ekwealor, I. A. (2016b). Effect of biosurfactant produced by *Citrobacter murliniae* AF025369 and a synthetic surfactant on degradation of crude oil. *Edorium Journal of Microbiology, 2*, 1–6.

Aslanzadeh, S., Kho, K., & Sitepu, I. (2020). An evaluation of the effect of Takakura and effective microorganisms (EM) as bioactivators on the final compost quality. *IOP Conference Series: Materials Science and Engineering, 742*, 012017. https://doi.org/10.1088/1757-899X/742/1/012017

Bhardwaj, K., Sharma, A., Tejwan, N., Bhardwaj, S., Bhardwaj, P., Nepovimova, E., Shami, A., Kalia, A., Kumar, A., Abd-Elsalam, K. A., et al. (2020). *Pleurotus* macrofungi-assisted nanoparticle synthesis and its potential applications: A review. *Journal of Fungi, 6*, 351.

Cai, Y., Li, C., Wu, D., Wang, W., Tan, F., Wang, X., Wong, P. K., & Qiao, X. (2017). Highly active MgO nanoparticles for simultaneous bacterial inactivation and heavy metal removal from aqueous solution. *Chemical Engineering Journal, 312*, 158–166.

Diachenko, O. V., Opanasuyk, A. S., Kurbatov, D. I., Opanasuyk, N. M., Kononov, O. K., Nam, D., & Cheong, H. (2016). Surface morphology, structural and optical properties of MgO films obtained by spray pyrolysis technique. *Acta Physica Polonica A, 130*, 805–810.

Duong, T. H. Y., Nguyen, T. N., Oanh, H. T., Dang Thi, T. A., Giang, L. N. T., Phuong, H. T., Anh, N. T., Nguyen, B. M., Tran Quang, V., Le, G. T., & Nguyen, T. N. (2020). Synthesis of magnesium oxide nanoplates and their application in nitrogen dioxide and sulfur dioxide adsorption. *Journal of Chemistry, 2*, 43.

Egurefa, S. O., Awari, V. G., Okinedo, J. I., Ogbonna, U. S. A., Obianom, A. O., Aniekwu, C. C., Agu, K. C., Umeoduagu, N. D., Nwosu, J. C., & Aji, S. M. (2024). Isolation and identification of fungal species in pesticide-contaminated soil from Abo-Obosi, Anambra. *Research Journal of Life Science, Bioinformatics, Pharmaceuticals and Chemical Sciences, 10*(5), 1–12.

Fazlzadeh, M., Rahmani, K., Zarei, A., Abdoallahzadeh, H., Nasiri, F., & Khosravi, R. (2016). A novel green synthesis of zero-valent iron nanoparticles using three plant extracts and their efficient application for removal of Cr(VI) from aqueous solutions. *Advanced Powder Technology.*

Fernandes, M., Singh, K. R. B., Sarkar, T., Singh, P., & Singh, R. V. (2020). Recent application of magnesium oxide nanoparticles in various domains. *Advanced Materials Letters, 11*(8).

Fouda, A., Hassan, S. E. D., Saied, E., & Hamza, M. F. (2021). Photocatalytic degradation of real textile and tannery effluent using biosynthesized magnesium oxide nanoparticles (MgO-NPs), heavy metal adsorption, phytotoxicity, and antimicrobial activity. *Journal of Environmental Chemical Engineering, 9*.

Hassan, S. E. D., Fouda, A., Saied, E., Farag, M. M. S., Eid, A. M., Barghoth, M. G., Awad, M. A., Hamza, M. F., & Awad, M. F. (2021). *Rhizopus oryzae*-mediated green synthesis of magnesium oxide nanoparticles (MgO-NPs): A promising tool for antimicrobial, mosquitocidal action, and tanning effluent treatment. *Journal of Fungi, 7*, 372.

Hornak, J. (2021). Synthesis, properties, and selected technical applications of magnesium oxide nanoparticles: A review. *International Journal of Molecular Sciences, 22*(23), 12752.

Jeevanandam, J., Chan, Y. S., & Danquah, M. K. (2017). Biosynthesis and characterization of MgO nanoparticles from plant extracts via induced molecular nucleation. *New Journal of Chemistry, 41*, 2800–2814.

Karanja, W., Njeru, E. M., & Maingi, J. M. (2019). Assessment of physicochemical changes during composting rice straw with chicken and donkey manure. *International Journal of Recycling of Organic Waste in Agriculture, 8*(Suppl. 1), S65–S72.

Kaul, R. K., Kumar, P., Burman, U., Joshi, P., Agrawal, A., Raliya, R., & Tarafdar, J. C. (2012). Magnesium and iron nanoparticles production using microorganisms and various salts. *Materials Science-Poland, 30*(3), 254–258.

Kazemi, M., Akbari, A., Zarrinfar, H., Soleimanpour, S., Sabouri, Z., Khatami, M., & Darroudi, M. (2020). Evaluation of antifungal and photocatalytic activities of gelatin stabilized selenium oxide nanoparticles. *Journal of Inorganic and Organometallic Polymers and Materials*. https://doi.org/10.1007/s10904-020-01462-4

Khan, A., Shabbier, D., Ahmad, P., Khandaker, M. U., Faruque, M. R. I., & Din, I. (2020). Biosynthesis and antibacterial activity of MgO nanoparticles produced from *Camellia sinensis* leaf extract. *Materials Research Express, 8*, 15402.

Limaye, L., Patil, R., Ranadive, P., & Kamath, G. (2017). Application of potent actinomycete strains for biodegradation of domestic agro-waste by composting and treatment of pulp-paper mill effluent. *Advances in Microbiology, 7*, 94–108.

Mbachu, A. E., Onochie, C. C., Agu, K. C., Okafor, O. I., & Awah, N. S. (2014). Hydrocarbon degrading potentials of indigenous bacteria isolated from auto-mechanic workshops at Mgbuka-Nkpor, Nigeria. *Journal of Global Biosciences, 3*(1), 321–326.

Namasivayam, S. K. R., Gnanendra, K. E., & Reepika, R. (2010). Synthesis of silver nanoparticles by *Lactobacillus acidophilus* 01 strain and evaluation of its in vitro genomic DNA toxicity. *Nano-Micro Letters, 2*(3), 160–163.

Nguyen, D. T. C., Dang, H. H., Vo, D. V. N., Bach, L. G., Nguyen, T. D., & Tran, T. V. (2021). Biogenic synthesis of MgO nanoparticles from different extracts of *Tecoma stans* and their utilization in organic dye treatment. *Journal of Hazardous Materials, 404*, 124146.

Ogbo, F., & Okonkwo, J. (2012). Some characteristics of a plant growth-promoting *Enterobacter* sp. isolated from the roots of maize. *Advances in Microbiology, 2*, 368–374.

Okeke, B. C., Uwanta, L. I., Odibo, F. J. C., Agu, K. C., & Victor-Aduloju, A. T. (2023). Monoculture solid-phase degradative potential of Congo red by *Aspergillus niger* and *Aspergillus flavus*. *International Journal of Trend in Scientific Research and Development, 7*(3), 684–688.

Opetubo, O., Shen, T., Bordia, R., & Aidhy, D. S. (2025). Fundamental understanding of oxygen vacancy energetics in rocksalt Mg(CuNiCoZn)O high entropy oxide from DFT and experiments. *Acta Materialia*, 121291.

Orji, M. U., Agu, K. C., Ikele, M. O., Uwanta, L. I., & Ugwuoke, G. (2022). Bioremediation of glyphosate-polluted soil using fungal species. *International Journal of Trend in Scientific Research and Development, 6*(7), 726–732. https://www.ijtsrd.com/papers/ijtsrd52396.pdf

Orji, M. U., Ezenekwe, F. N., Odibo, F. J. C., Agu, K. C., & Mbachu, A. E. (2014). Utilization of used global system for mobile communication (GSM) recharge cards for cellulase production by *Penicillium* species and *Aspergillus* species. *American Journal of Life Science Researches, 2*(4), 548–556.

Pugazhendhi, A., Prabhu, R., Muruganantham, K., Shanmuganathan, R., & Natarajan, S. (2019). Anticancer, antimicrobial and photocatalytic activities of green synthesized magnesium oxide nanoparticles using aqueous extract of *Sargassum wightii*. *Journal of Photochemistry and Photobiology B: Biology, 190*, 86–97.

Pushpa, T. B., Sekaran, V., Basha, S. J. S., & Jegan, J. (2016). Investigation on preparation, characterization and application of effective microorganisms (EM)-based composts: An eco-friendly solution. *Nature Environment and Pollution Technology, 15*(1), 153–158.

Saied, E., Eid, A. M., Hassan, S. E. D., Salem, S. S., Radwan, A. A., Halawa, M., Saleh, F. M., Saad, H. A., Saied, E. M., & Fouda, A. (2021). The catalytic activity of biosynthesized magnesium oxide nanoparticles (MgO-NPs) for inhibiting the growth of pathogenic microbes, tanning effluent treatment, and chromium ion removal. *Catalysts, 11*, 821.

Saleh, Z. M. D., Mohamed, R. M. S. R., Al-Gheethi, A., Zainun, N. Y., & Kamil, N. A. F. M. (2020). Optimizing decomposition of food wastes using response surface methodology. *Materials Today: Proceedings.* https://doi.org/10.1016/j.matpr.2020.01.251

Umeh, S. O., Okpalla, J., & Okafor, J. N. C. (2019). Novel sources of *Saccharomyces* species as leavening agent in bread making. *International Journal of Trend in Scientific Research and Development, 3*(2), 827–831.

Wang, T., Jin, X., Chen, Z., Megharaj, M., & Naidu, R. (2014). Green synthesis of Fe nanoparticles using eucalyptus leaf extracts for treatment of eutrophic wastewater. *Science of the Total Environment, 466–467*, 210–213.

Zhang, C., Xiao, G., Peng, L., Su, H., & Tan, T. (2013). Anaerobic co-digestion of food waste and cattle manure. *Bioresource Technology, 129*, 170–176.

Zhao, K., Xu, R., Zhang, Y., Tang, H., Zhou, C., Cao, A., Zhao, G., & Guo, H. (2017). Development of a novel compound microbial agent for the degradation of kitchen waste. *Brazilian Journal of Microbiology, 48*, 442–450.